

I dont know yet



Faustmann Christian

Faculty of Physics
Technical University of Vienna

This thesis is submitted for the degree of
Bachelor of Science

Introduction

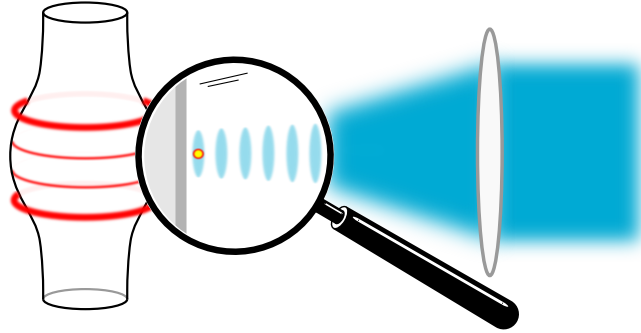


Fig. 1 Schematic representation of a WGM resonator and an optical dipole trap

One of Prof. Rauschenbeutel's projects uses a novel type of whispering-gallery-mode (WGM) resonator interfaced via nanowaveguides and coupled to single Rubidium atoms to carry out experiments in the realm of Cavity Quantum Electrodynamics. The WGM resonator is a so-called bottle-microresonator (BMR) manufactured from a standard optical glass fiber in a heat and pull process. The light is radially confined inside the resonator by total internal reflection and propagates along the circumference of the resonator. In such a structure, a significant fraction of the light field propagates in the evanescent field. By overlapping this field with the evanescent field of an optical nanofiber, light can be coupled into and out of the resonator very efficiently. Due to the extremely low absorption of silica (and low surface roughness) we can produce bottle-resonators with ultra-high optical Q-factor exceeding 10^8 . Rubidium atoms are delivered to the resonator using an atomic fountain. When the atoms enter the vicinity of the WGM, and they are in the evanescent field they can be strongly coupled to the light. For the moment the ^{85}Rb atoms are only flying by the resonator for $\sim 2\mu\text{s}$. Moreover the distance between the resonator and the atom is not controlled. This uncertainty induces fluctuations on the atom-resonator coupling from shot to shot and limits the efficiency of the different devices demonstrated with the setup. The short duration of the atom light interaction also prevents the manipulation of the atomic state, necessary for the realization of complex quantum information protocols such as two photon gates [1]. The solution would be to trap the atom at the vicinity of the BMR. The choice made to trap

the atom is to use a dipole trap created from the retroreflection of a focused beam on the resonator surface inspired from [2] (see Fig. 1). Due to the experiment configuration, the trap can not be loaded from a dense cloud, but only from the atoms flying next to the resonator, which have a non-zero velocity, which further implies that a big trap depth is needed. The usual dipole traps are built with lasers detuned from the transition between the ground and the first excited state. But this would create a trap too far from the resonator and thus in this thesis, we discuss the possibility to realise a trap detuned from the second excited state of ^{85}Rb which has transitions at $\lambda \approx 420\text{ nm}$.

Table of contents

List of figures	vii
List of tables	ix
1 Theory of laser trapping of atoms	1
2 Absorption of photon by an atom	7
2.1 Laser interactions - Two-level atom	7
2.2 The $5S_{1/2} \rightarrow 6P_{3/2}$ transition of ^{85}Rb	8
2.3 Laser absorption spectroscopy	9
2.4 Equation	10
2.5 Doppler shifts	10
2.6 Absorption coefficient - weak field	11
2.7 Population	13
2.8 Absorption coefficient - general case	15
2.9 Non-linear differential equation	16
2.10 Data table	17
2.11 D2 line	18
3 Experiment	21
3.1 Setup & Tools	21
3.2 Laser diameter measurement	21
3.3 Power / intensity measurement	21
3.4 Doppler-free measurement	21
4 Evaluation	23
4.1 Data processing	23
4.2 Temperature & saturation intensity	23
4.3 Comparison with theory	23
4.4 Compare Doppler-free measurement with theoretical values	23

References

25

List of figures

1	Schematic representation of a WGM resonator and a optical dipole trap . . .	iii
1.1	Illustration of dipole traps with red and blue detuning. The grey area represents regions of high intensity.	1
1.2	1D Intensity distribution of a retroreflected gaussian laser beam for a partial standing wave with $r = -0.2$	2
1.3	Level scheme of ^{85}Rb with lifetimes and transition wavelength of the first states.	3
1.4	Experimental setup and intensity distribution.	4
1.5	Overlap of dipole and Van-der-Waals potential.	5
1.6	Trap depth for different detuning.	5
1.7	Calculated trap potential for 20 mW power and a 6 GHz detuning.	6
2.1	Two-level atom model	8
2.2	The Lorentzian line shape profile for a transition	9
2.3	Basic arrangement for ordinary laser absorption spectroscopy.	9
2.4	The Lorentzian compared to the Gaussian profile	12
2.5	$5^2S_{1/2} \rightarrow 6^2P_{3/2}$ transition of ^{85}Rb and ^{87}Rb with corresponding hyperfine structure	18
2.6	Doppler spectrum of D2 line	18
2.7	Relative energy gaps of the groundstates between both isotopes	19

List of tables

2.1	Properties of rubidium isotopes	17
-----	---	----

Chapter 1

Theory of laser trapping of atoms

Atoms can be trapped in an optical potential created by the dispersive interaction of the atomic dipole moment with the intensity gradient of the light field. These trap can be used to confine the atoms in 3D counteract gravity. In the case of large detunings the expressions for the dipole potential and scattering rate[3] are the following:

$$U_{\text{dip}}(z) = \frac{3\pi c^2}{2\omega_0^3} \frac{\Gamma}{\Delta} I(z) , \quad (1.1)$$

$$\Gamma_{\text{sc}}(z) = \frac{3\pi c^2}{2\hbar\omega_0^3} \left(\frac{\Gamma}{\Delta} \right)^2 I(z) . \quad (1.2)$$

Where c is the speed of light, Γ is the coupling strength between the two atomic levels of the atomic transition, Δ is the detuning between the light and the atomic transition ($\Delta := \omega - \omega_0$), where ω is the driving pulsation of the light field and ω_0 the atomic transition pulsation $\omega_0 = 2\pi \frac{c}{\lambda_0} = 2\pi\nu_0$ and $I(z)$ corresponds to the intensity of the light field at a distance from the resonator. Dipole traps can be divided into two main classes, red-detuned traps ($\Delta < 0$) and blue-detuned traps ($\Delta > 0$). Below an atomic resonance (red) the dipole potential is negative and the potential minima are therefore found at positions of maximum intensity. For a blue-detuned light the potential minima correspond to minima of the intensity and the interaction repels atoms from the field as seen in Fig. 1.1. For our setup we will consider a red-detuned trap.

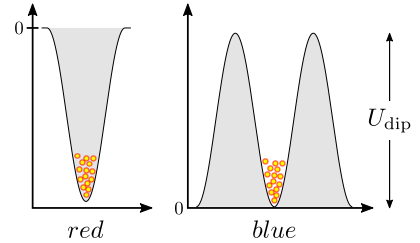


Fig. 1.1 Illustration of dipole traps with red and blue detuning. The grey area represents regions of high intensity.

There are three different trap configurations possible:

- *focused-beam trap*: Focused-beam traps are consisting of a single strongly focused beam and have a confinement volume proportional to $z_R \times w_0^2$, where z_R is the Rayleigh length and w_0 is the beam radius.
- *crossed-beam trap*: A crossed-beam configuration uses two or more beams which intersect at their foci. The confinement volume reduces to the intersection of the contributing beams, which is in case of w_0 smaller than w_1 the cross section of “beam 0” times the diameter of “beam 1”.
- *standing wave trap*: In case of a standing wave trap the atoms are axially confined in the antinodes of a standing wave. If the standing wave is created through a retroreflection the first antinode and therefore first trapping site lies at a distance of $\frac{\lambda}{4}$ from the surface (see Fig. 1.2). The resulting volume is in the order of $w_0^2 \times \frac{\lambda}{4}$.

For our Experiment it is important that the atoms are as close as possible from the resonator, because the interacting evanescent field of the photon in the resonator decreases exponentially with a decay length of $\frac{\lambda_{at}}{2\pi}$ where λ_{at} is the wavelength of the cavity field tuned to the atomic transition. $5S_{1/2} \rightarrow 5P_{3/2}$ (D_2 line of Rb at 780 nm) has a decay length of 124 nm.

If one uses a laser closely detuned from the D_2 line $5S_{1/2} \rightarrow 5P_{3/2}$, i.e. 780 nm, this leads to a distance of $\frac{\lambda}{4} \approx 190$ nm. This would be too far from the resonator which is already too far. Rubidium atoms also have a transition from $5S_{1/2}$ to $6P_{3/2}$ at 420 nm. The transition strength are much weaker for this line, and the aim of this thesis is to decide on the feasibility of such a trap and as the case may be determine the parameters for it.

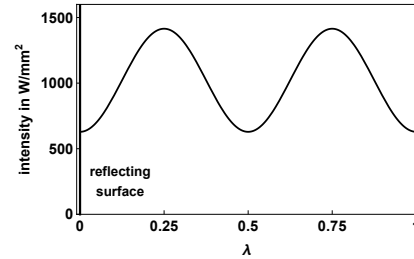


Fig. 1.2 1D Intensity distribution of a retroreflected gaussian laser beam for a partial standing wave with $r = -0.2$.

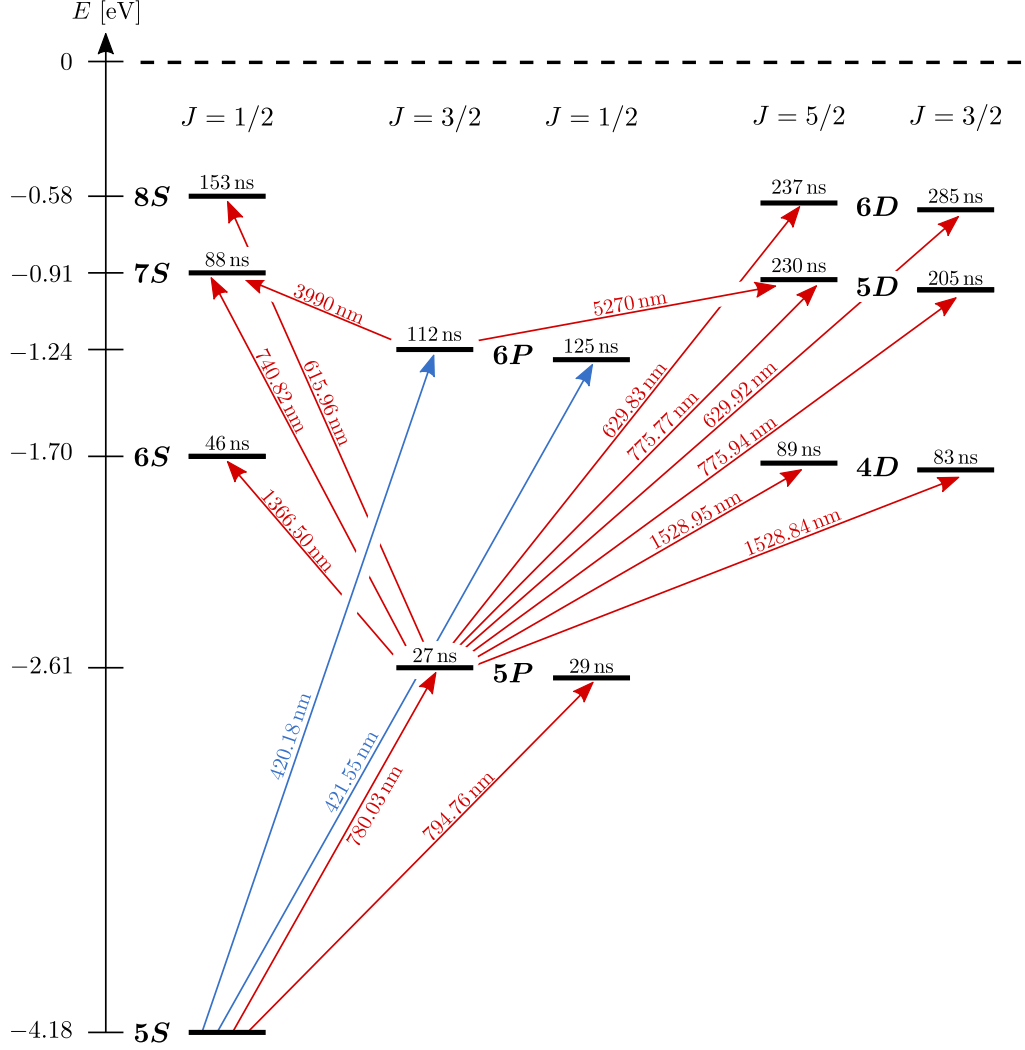


Fig. 1.3 Level scheme of ^{85}Rb with lifetimes and transition wavelength of the first states.

As we can see in Eq. (1.1) the dipole potential is proportional to $\frac{I}{\Delta}$, which means that we have two degrees of freedom, the detuning and the power ($I \propto \frac{P}{\text{crosssection}}$). To choose our parameters properly we have to consider some constraints. We want to keep the scattering rate as low as possible, because each photon scattered may depolarize the atom or also lead to depump the atom in which case it cannot be detected anymore. The scattering rate is proportional to $\frac{I}{\Delta^2}$ (Eq. 1.2), so a detuning as big as possible would be beneficial. On the other hand laser power is limited ($P_{\text{max}} = 80 \text{ mW}$), due to the maximum power output of our laser. And additionally we do not want to send too much power onto the resonator, because due to the highly focused beam ($w_0 = 3.6 \mu\text{m}$) and the more energetic wavelength the resonator could be damaged. To compensate the lower laser power the detuning has to be small. However if Δ smaller than the separation between the D_1 and D_2 lines (420 & 421 nm) then we need to

take the fine structure of the atom into account and equations (1.1) and (1.2) rewrite as

$$U_{\text{dip}}(z) = \frac{\pi c^2}{2\omega_0^3} \left(\frac{2 \Gamma_{\omega,D2}}{\Delta_{D2}} + \frac{\Gamma_{\omega,D1}}{\Delta_{D1}} \right) I(z) , \quad (1.3)$$

$$\Gamma_{\text{sc}}(z) = \frac{\pi c^2}{2\hbar\omega_0^3} \left(\frac{2 \Gamma_{\omega,D2} \Gamma_{\omega,D2,tot}}{\Delta_{D2}^2} + \frac{\Gamma_{\omega,D1} \Gamma_{\omega,D1,tot}}{\Delta_{D1}^2} \right) I(z) . \quad (1.4)$$

It should be noted that as $6P_{1/2}$ and $6P_{3/2}$ are not the first excited states, there exist several possible decay channels from there to the ground state. $\Gamma_{\omega,Dx}$ are the transition strength from $5S_{1/2} \rightarrow 6P_{1/2}$ and $5S_{1/2} \rightarrow 6P_{3/2}$, while $\Gamma_{\omega,Dx,tot}$ are total decay rates of the $6P_{1/2}$ and $6P_{3/2}$ states with $\frac{1}{\Gamma_{\omega,Dx,tot}}$ the mean lifetime of the state and Δ_{Dx} represents $\omega - \omega_{0,Dx}$. All values can be found in table 2.1. In our case we are red-detuned from the D_2 -transition and the detuning will be smaller than the fine structure splitting of 2.32 THz, so we get an additional counter term of the D_1 -transition (blue-detuned).

It should be noted that $\Gamma_{6P_{3/2}}$ is 20 times weaker than $\Gamma_{5P_{3/2}}$ and thus, for the same trap depth a shorter detuning or higher power will be needed comparatively to a dipole trap around 780 nm.

Possible configuration of optical dipole trap

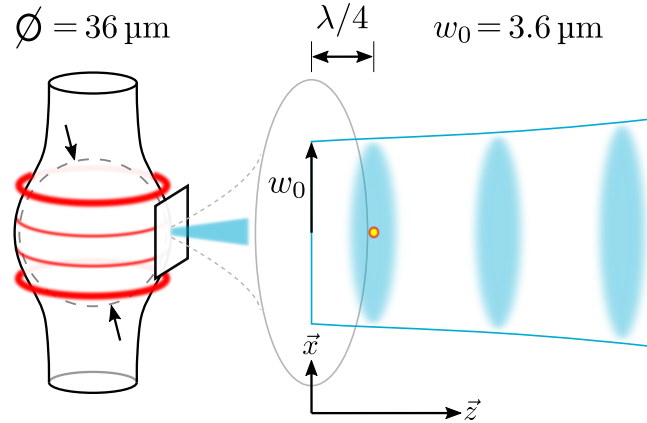


Fig. 1.4 Experimental setup and intensity distribution.

To calculate the trap potential we have to derive the intensity of the standing wave. The trap is produced by a beam focused down to at radius of $w_0 = 3.6 \mu\text{m}$. While the resonator diameter is $36 \mu\text{m}$ (as shown in Fig. 1.4). Thus, one can consider that the beam is retroreflected on a planar surface. With this assumption the electric field becomes:

$$\vec{E}(z) = E_0 \vec{x} \left(e^{-ik_z z} + r e^{ik_z z} \right) \quad (1.5)$$

with r as the reflection coefficient in amplitude, which is in case of a glass/vacuum interface $r = -0.2$. k_z is the wave vector in z-direction and equal to $\frac{2\pi}{\lambda}$. This leads to the intensity

$$I(z) = \frac{2|\vec{E}(z)|^2}{\eta} \quad (1.6)$$

depicted in Fig. 1.2. Where η is the characteristic impedance and $\frac{2E_0^2}{\eta}$ will be denoted as the maximum intensity I_0 . Related to the power of a gaussian beam as

$$P_0 = \frac{1}{2} I_0 w_0^2 \pi . \quad (1.7)$$

The range of power accessible is between $0 < P_0 < 80 \text{ mW}$, due the maximum laser output power.

The trap depth must be bigger than the energy of the atom, here the kinetic energy $E_{kin} = \frac{1}{2} m_R b v^2$ due to the fact that the atoms are free falling up to 60 ms. It corresponds in terms of temperature to $E_{kin}/k_B = 1.77 \text{ mK}$. Our trap is conservative. When an atom is captured it gains the potential energy at its position $E_{pot}(z)$ and if $E_{kin} + E_{pot}(z)$ less than $E_{pot,max}$ then the atom will not be trapped. Therefore one should add a safety margin to capture more atoms. For example a 5 mK trap would capture $\frac{5-1.77}{5} \approx 60 \%$ of atoms entering the trap in the worst case. In our setup we are so close to the resonator that the atoms are also sensitive to the Van-der-Waals potential[4]

$$U_{VdW} = -\frac{C_3}{r^3} \quad (1.8)$$

(see Fig. 1.5). The C_3 coefficient is $h \cdot 770 \cdot 10^{-18} \text{ Hz m}^3$ [5], where h is Plank's constant.

The total potential seen by the atoms is $U_{VdW} + U_{dip}$. The depth of the potential well is now the difference

between the reduced first maximum and the first minimum at $\lambda/4$. For our trap we expect to have 20 mW of laser power accessible. The power losses include locking the laser to a fixed frequency (5 mW), because the frequency deviation in free running can be on the order of 1 GHz when we need to be only 10 GHz from resonance away (see. Fig. 1.6). One also needs to take into account the losses due to the optical path of the beam before reaching the atoms, which will contain acousto-optical modulators (AOMs) and fiber coupling. As we can see in

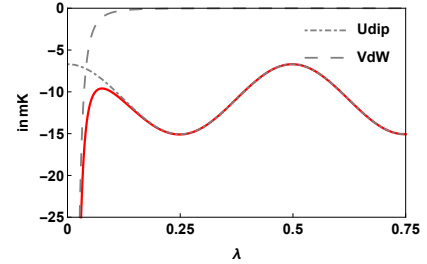


Fig. 1.5 Overlap of dipole and Van-der-Waals potential.

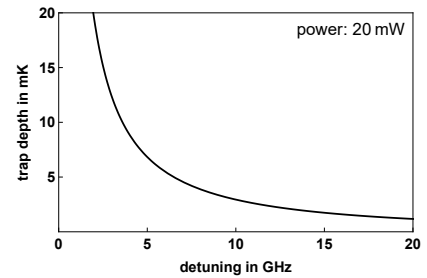


Fig. 1.6 Trap depth for different detuning.

Fig. 1.6 for 20 mW power the detuning has to be lower than 7 GHz. For a detuning of 6 GHz we get a trap depth of 5.5 mK as shown in Fig. 1.7.

In order to set the laser detuning properly, we need to realize a spectroscopy on the $5S_{1/2} \rightarrow 6P_{3/2}$ transition. (see Chapter 3)

As seen above in all the formulas to calculate the trap depth the transition strength plays a significant role. To be sure we are using the right value we will measure it in our lab. For that we will measure the related intensity saturation of the $5S_{1/2} \rightarrow 6P_{3/2}$ transition. It marks the point where excited state atoms are equally likely to decay by stimulated emission or by spontaneous emission. Afterwards we can check with a theoretical relation where every other value is known, if the value is correct.

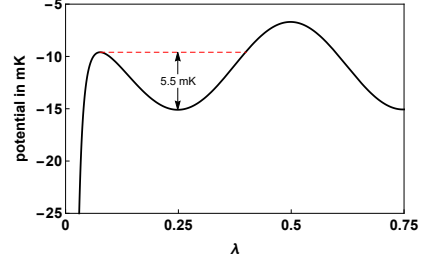


Fig. 1.7 Calculated trap potential for 20 mW power and a 6 GHz detuning.

$$I_{s,420} = \frac{\Gamma_{\omega,tot,420} \cdot \omega_{420}^3 \cdot I_{s,780}}{\Gamma_{\omega,420} \cdot \Gamma_{\omega,780} \cdot \omega_{780}^3} \quad (1.9)$$

The index 420 corresponds to $5S_{1/2} \rightarrow 6P_{3/2}$ and the index 780 to $5S_{1/2} \rightarrow 5P_{3/2}$. (see Chapter 4) In the next chapter we will discuss how atoms affect laser photon in order to perform a absorption spectroscopy.

Chapter 2

Absorption of photon by an atom

The purpose of this section is to outline the basic features observed in saturated absorption spectroscopy and relate them to simple atomic and laser physics principles. For this we will follow the guidance of [6] and [7].

Electrons can orbit around the atom nucleus following different trajectories which are quantified, the so called orbitals. It is energetically preferable that the electron orbit around the atomic nucleus in the lowest possible orbitals, but it is possible to excite the electron in different higher excited states. The difference of energy states are in the range of typically optical frequencies, which give rise to absorption spectrum. The atomic transitions are sufficiently separated such that, when probing close to one resonance, one can consider that they behave as a 2 level system.

2.1 Laser interactions - Two-level atom

We begin with the interaction between a laser field and a sample of stationary atoms having only two possible energy levels. Aspects of thermal motion will be treated subsequently.

The ground state is denoted $|g\rangle$ of energy E_0 and the excited state $|e\rangle$ of energy E_1 . The frequency ν_0 of the transition given by Planck's law

$$h\nu_0 = E_1 - E_0 = \Delta E . \quad (2.1)$$

For the considered transition ν_0 is in the optical domain. There are three types of transition processes and a light field:

- (1) *absorption*: Atom in the ground state absorbs a photon with the energy ΔE and is excited. The absorption rate Γ_ω equals the rate at which the atom is excited and corresponds to the linewidth of the transition.
- (2) *spontaneous emission*: The excited state has a finite lifetime τ corresponding to $\frac{1}{\Gamma}$, the width of the transition. The atom will decay to its ground state following an exponential statistics of rate τ , by emitting a photon of energy $h\nu_0$ in any possible direction of space and any polarization.

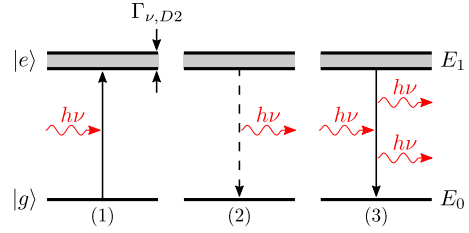


Fig. 2.1 Two-level atom model

- (3) *stimulated emission*: If a photon of $h\nu_0$ impinges on an atom in the excited state, the atom will “deexcite” by emitting a photon which has the same characteristics (\vec{k} , phase, polarization) of the incident photon.

For a real two-level atom the rate of absorption Γ_ω is equal to the rate of spontaneous emission and the rate of stimulated emission.

2.2 The $5S_{1/2} \rightarrow 6P_{3/2}$ transition of ^{85}Rb

The main difference is that the spontaneous emission rate is different to the real two-level atom $\Gamma_{\omega,tot} = \frac{1}{\text{lifetime of excited state}}$. But absorption and stimulated emission correspond to $\Gamma_{transition}$, because the photon emitted or absorbed correspond to this line at 420 nm with $\Gamma_{D2} = 2\pi \times 0.282 \text{ MHz}$.

We want to probe the $5S_{1/2} \rightarrow 6P_{3/2}$ transition, which is not the lowest energy transition. Thus when the atom is in the $6P_{3/2}$ state it has several decay channels (e.g. $6P_{3/2} \rightarrow 6S_{1/2} \rightarrow 5P_{3/2} \rightarrow 5S_{1/2}$). Therefore the lifetime of the state $\tau = 112 \text{ ns} = \frac{1}{\Gamma_{tot}} \neq \frac{1}{\Gamma_{transition}}$.

So, in the absence of an external field, any initial population of excited state atoms would decay exponentially to the ground state with a mean life time $\Delta t = 1/\Gamma_{\omega,tot} \approx 122 \text{ ns}$. In the rest frame of the atom, spontaneous photons are emitted in all directions with an energy spectrum having a mean $E = h\nu_0$ and a full width at half maximum (FWHM) ΔE given by the Heisenberg uncertainty principle $\Delta E \Delta t = \hbar$ or $\Delta E = \Gamma_{\omega,tot} \hbar$. Expressed in frequency units, the FWHM is called the *natural linewidth* and given the symbol $\Gamma_{\nu,tot}$. Thus

$$\Gamma_{\nu,tot} = \frac{\Gamma_{\omega,tot}}{2\pi} \quad (2.2)$$

For the $6P_{3/2}$ state $\Gamma_\nu \approx 0.282$ MHz.

The stimulated emission and absorption processes are also described by a transition rate – a single rate giving the probability per unit time for a ground state atom to absorb a laser photon or for an excited state atom to emit a laser photon. The absorption and stimulated transition rate is proportional to the laser intensity I (SI units of W m^{-2}) and is only significantly different from zero when the laser frequency ν is near the resonance frequency ν_0 . This transition rate will be denoted αI , where

$$\alpha = \alpha_0 \mathcal{L}(\nu, \nu_0) \quad (2.3)$$

and

$$\mathcal{L}(\nu, \nu_0) = \frac{1}{1 + 4(\nu - \nu_0)^2 / \Gamma_\nu^2} \quad (2.4)$$

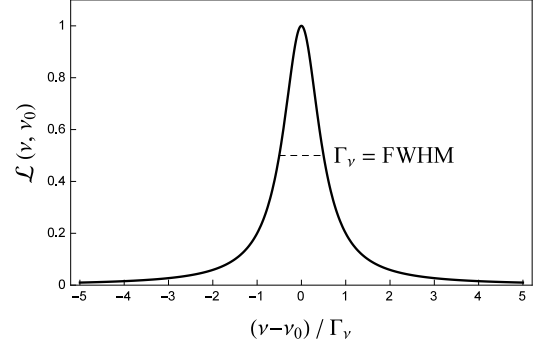


Fig. 2.2 The Lorentzian line shape profile for a transition

gives the *Lorentzian* frequency dependence as shown in Fig. 2.2. The maximum transition rate $\alpha_0 I$ occurs right on resonance ($\nu = \nu_0$).

An important value is

$$I_s = \frac{\Gamma_\omega}{\alpha_0} \quad (2.5)$$

which defines the saturation intensity of an atom and a specific state. Its significance is that when the laser intensity is equal to the saturation intensity, excited state atoms are equally likely to decay by stimulated emission or by spontaneous emission.

2.3 Laser absorption spectroscopy

The arrangement for ordinary laser absorption spectroscopy through a gaseous sample is shown in Fig. 2.3. A laser beam passes through the vapor cell and its intensity is measured by a photodiode detector as the laser frequency ν is scanned through the resonance frequency of a atomic transition.

To get a better understanding of absorption spectroscopy we will establish the basic equation describing how the laser intensity changes as it propagates through the sample and then we will incorporate with the effects of Doppler shifts and population changes.

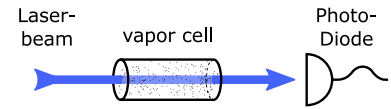


Fig. 2.3 Basic arrangement for ordinary laser absorption spectroscopy.

2.4 Equation

When a laser beam propagates through a gaseous sample, absorption and stimulated emission change the intensity of the laser beam and affect the proportion of atoms in the ground and excited states. The laser intensity $I(x)$ varies from x to $x + dx$ in the medium as follows:

$$I(x + dx) - I(x) = -\alpha I(x) h\nu n_0 (P_0 - P_1) dx \quad (2.6)$$

where $\alpha I(x)$ is the transition rate, as discussed before, n_0 the atom density and $P_{0,1}$ are the probability that the atom is in the ground or in the excited state.

Equation 2.6 leads to

$$\frac{dI}{dx} = -\kappa I \quad (2.7)$$

where the *absorption coefficient* (fractional absorption per unit length)

$$\kappa = \alpha h\nu n_0 (P_0 - P_1) \quad (2.8)$$

It should be noted that the proportionality to $P_0 - P_1$ arises from the competition between stimulated emission and absorption and it is important to appreciate the consequences. If there are equal numbers of atoms in the ground and excited state ($P_0 - P_1 = 0$), laser photons are as likely to be emitted by an atom in the excited state as they are to be absorbed by an atom in the ground state and there will be no attenuation of the incident beam. The attenuation maximizes when all atoms are in the ground state ($P_0 - P_1 = 1$) because only absorption is possible. And the attenuation can even reverse sign (become an amplification as it does in laser gain media) if there are more atoms in the excited state ($P_0 > P_1$).

2.5 Doppler shifts

Atoms in a vapor cell move randomly in all three directions with a velocity distribution dependent on the temperature. Only the component of velocity parallel to the laser beam direction will be important when taking into account Doppler shifts and it is this component we refer to with the symbol v . The density of atoms dn in having a velocity comprised between v and $v + dv$ is given by the Boltzmann velocity distribution:

$$dn = n_0 \sqrt{\frac{m}{2\pi k_B T}} \exp\left(-\frac{m v^2}{2 k_B T}\right) dv \quad (2.9)$$

defining the standard deviation

$$\sigma_v = \sqrt{\frac{k_B T}{m}} \quad (2.10)$$

It can be rewritten using the canonical form of a Gaussian distribution

$$dn = n_0 \frac{1}{\sqrt{2\pi} \sigma_v} \exp\left(-\frac{v^2}{2 \sigma_v^2}\right) dv \quad (2.11)$$

with a mean of zero – indicating the atoms are equally likely to be going in the positive or negative z direction, i.e. they have positive or negative velocities. It is properly normalized so that the integral over all velocities ($-\infty \rightarrow \infty$) is n_0 , the overall atom density.

Atoms moving with a velocity v see the laser beam Doppler shifted by the amount $\nu(v/c)$. This corresponds to a Doppler shifted resonance frequency

$$\nu'_0 = \nu_0 \left(1 + \frac{v}{c}\right) \quad (2.12)$$

in the lab frame. The sign has been chosen for a laser beam propagating in the positive direction so that the resonance frequency is blue shifted to higher frequencies if v is positive and red shifted if v is negative.

The absorption coefficient $d\kappa$ from a velocity group dn at a laser frequency ν is then obtained from Eq. 2.8 by substituting dn for n_0 and by adjusting the Lorentzian dependence of α so that it is centered on the Doppler shifted resonance frequency ν'_0 (Eq. 2.12).

$$d\kappa = \alpha_0 h\nu (P_0 - P_1) \mathcal{L}(\nu, \nu'_0) dn \quad (2.13)$$

The absorption coefficient from all atoms is then found by integrating over all velocity classes.

2.6 Absorption coefficient - weak field

We consider the weak-laser intensity case, where we have a very low intensity compared to I_s and therefore nearly all atoms will be in the ground state, i.e., $P_0 - P_1 = 1$ so that

$$d\kappa = \alpha_0 h\nu n_0 \frac{1}{\sqrt{2\pi} \sigma_v} \mathcal{L}(\nu, \nu'_0) \exp\left(-\frac{v^2}{2\sigma_v^2}\right) dv \quad (2.14)$$

and

$$\kappa = \underbrace{\alpha_0 h\nu n_0}_{\beta} \frac{1}{\sqrt{2\pi} \sigma_v} \int_{-\infty}^{\infty} \frac{1}{1 + 4 [\nu - \nu_0 (1 + \frac{v}{c})]^2 / \Gamma_\nu^2} \exp\left(-\frac{v^2}{2 \sigma_v^2}\right) dv \quad (2.15)$$

After the variable transformation

$$\left| \begin{array}{l} \nu'_0 = \nu_0 \left(1 + \frac{v}{c}\right) \\ v = \left(\frac{\nu'_0}{\nu_0} - 1\right) c \\ dv = \frac{c}{\nu_0} d\nu'_0 \end{array} \right| = \beta \frac{c}{\nu_0} \int_{-\infty}^{\infty} \frac{1}{1 + 4 (\nu - \nu'_0)^2 / \Gamma_\nu^2} \exp \left(-\frac{(\nu'_0 - \nu_0)^2 c^2}{2 \nu_0^2 \sigma_v^2} \right) d\nu'_0$$

and substitution $\sigma_\nu = \frac{\nu_0}{c} \sigma_v$ we get

$$\kappa = \beta \frac{c}{\nu_0} \int_{-\infty}^{\infty} \frac{1}{1 + 4 (\nu - \nu'_0)^2 / \Gamma_\nu^2} \exp \left(-\frac{(\nu'_0 - \nu_0)^2}{2 \sigma_\nu^2} \right) d\nu'_0 \quad (2.16)$$

Now we compare the width parameters from the Lorentzian (see table 2.1) with the Gaussian function and at room temperature (20 °C) (see Fig. 2.4):

$$\sigma_\nu = \frac{c}{\lambda_{D2}} \sqrt{\frac{k_B T}{m_{Rb85} c^2}} \approx 403 \text{ MHz}$$

$$\Gamma_{\nu, D2} = 0.282 \text{ MHz}$$

$$\Rightarrow \Gamma_{\nu, D2} \ll 2 \cdot \sigma_\nu$$

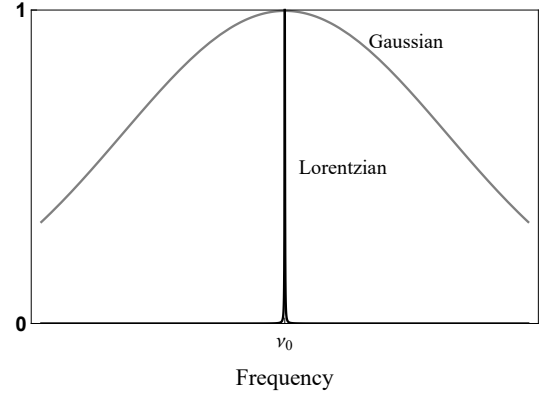


Fig. 2.4 The Lorentzian compared to the Gaussian profile

As we can see the Lorentzian function is significantly different from zero only within a very narrow range. Consequently the Gaussian remains relatively constant over the width of $\Gamma_{\nu, D2}$. Therefore Eq. (2.16) can be accurately determined as the integral of the Lorentzian times the value of the exponential at $\nu'_0 = \nu$:

$$= \beta \frac{c}{\nu_0} \exp \left(-\frac{(\nu - \nu_0)^2}{2 \sigma_\nu^2} \right) \int_{-\infty}^{\infty} \frac{1}{1 + 4 (\nu - \nu'_0)^2 / \Gamma_\nu^2} d\nu'_0 \quad (2.17)$$

and with the solution of the Lorentzian integral

$$\int_{-\infty}^{\infty} \mathcal{L}(\nu, \nu'_0) d\nu'_0 = \frac{\pi \Gamma_\nu}{2} \quad (2.18)$$

we finally get the absorption coefficient in a weak field

$$\kappa = \kappa_0 \exp\left(-\frac{(\nu - \nu_0)^2}{2 \sigma_\nu^2}\right) \quad \text{with} \quad \kappa_0 = \alpha_0 \frac{h\nu}{\sqrt{2\pi} \sigma_\nu} n_0 \frac{\pi \Gamma_\nu}{2} \quad (2.19)$$

2.7 Population

To determine the general case of the absorption coefficient we need to determine $P_0 - P_1$. For that we have to take into account the changes to the ground and excited state populations arising from a laser beam propagating through the cell. The rate equations for the ground and excited state are therefore:

$$\begin{aligned} \frac{dP_0}{dt} &= \Gamma_{\omega,tot} P_1 - \alpha I (P_0 - P_1) \\ \frac{dP_1}{dt} &= -\Gamma_{\omega,tot} P_1 + \alpha I (P_0 - P_1) \end{aligned} \quad (2.20)$$

where the first term on the right in each equation arises from spontaneous emission and the second term arises from absorption and stimulated emission.

With the additional equation $P_0 + P_1 = 1$ and the steady state condition

$$\frac{dP_0}{dt} = \frac{dP_1}{dt} = 0 \quad (2.21)$$

we get for the populations

$$P_0 = \frac{\Gamma_{\omega,tot} + \alpha I}{\Gamma_{\omega,tot} + 2\alpha I} ; \quad P_1 = \frac{\alpha I}{\Gamma_{\omega,tot} + 2\alpha I} \quad (2.22)$$

which leads to

$$(P_0 - P_1) = \frac{\Gamma_{\omega,tot}}{\Gamma_{\omega,tot} + 2\alpha I} \quad (2.23)$$

As we can see the population difference is dependent on $\Gamma_{\omega,tot}$ (spontaneous decay rate), which is related to the *Lorentzian width parameter*. To combine the Lorentzians in α (Eq. 2.3) and $(P_0 - P_1)$ we will define $\Delta\nu = 2(\nu - \nu_0)$:

$$\alpha = \alpha_0 \frac{1}{1 + \Delta\nu^2/\Gamma_\nu^2} = \alpha_0 \frac{\Gamma_\nu^2}{\Gamma_\nu^2 + \Delta\nu^2} ; \quad (P_0 - P_1) = \frac{2\pi \Gamma_{\nu,tot}}{2\pi \Gamma_{\nu,tot} + 2\alpha I} \quad (2.24)$$

and get

$$(P_0 - P_1)\alpha = \frac{2\pi \Gamma_{\nu,tot}}{2\pi \Gamma_{\nu,tot} + 2I \alpha_0 \frac{\Gamma_\nu^2}{\Gamma_\nu^2 + \Delta\nu^2}} \alpha_0 \frac{\Gamma_\nu^2}{\Gamma_\nu^2 + \Delta\nu^2} = \frac{\alpha_0 \pi \Gamma_\nu^2 \Gamma_{\nu,tot}}{\pi \Gamma_{\nu,tot} (\Gamma_\nu^2 + \Delta\nu^2) + I \alpha_0 \Gamma_\nu^2} \quad (2.25)$$

dividing with $\pi\Gamma_\nu$ and substitute in the denominator α_0 with the definition of Eq. (2.2) and (2.5) leads to

$$(P_0 - P_1)\alpha = \alpha_0 \frac{1}{1 + \frac{\Delta\nu^2}{\Gamma_\nu} + \frac{2I}{I_s} \frac{\Gamma_\nu}{\Gamma_{\nu,tot}}} = \frac{\alpha_0}{(1 + \frac{2I}{I_s} \frac{\Gamma_\nu}{\Gamma_{\nu,tot}})} \frac{1}{1 + \frac{\Delta\nu^2}{\Gamma_\nu^2 \left(1 + \frac{2I}{I_s} \frac{\Gamma_\nu}{\Gamma_{\nu,tot}}\right)}} \quad (2.26)$$

with the definition of the power-broadened *width parameter*

$$\Gamma'_\nu = \Gamma_\nu \sqrt{1 + \frac{2I}{I_s} \frac{\Gamma_\nu}{\Gamma_{\nu,tot}}} \quad (2.27)$$

we obtain

$$(P_0 - P_1)\alpha = \frac{\alpha_0}{\left(1 + \frac{2I}{I_s} \frac{\Gamma_\nu}{\Gamma_{\nu,tot}}\right)} \mathcal{L}'(\nu, \nu_0) \quad \text{and} \quad \mathcal{L}'(\nu, \nu_0) = \frac{1}{1 + \frac{4(\nu - \nu_0)^2}{\Gamma_\nu'^2}} \quad (2.28)$$

2.8 Absorption coefficient - general case

For the general case we take now into account the velocity groups and their corresponding Doppler shifts for the case $P_0 - P_1 \neq 1$ and therefore

$$d\kappa = h\nu n_0 \frac{\alpha_0}{(1 + \frac{2I}{I_s} \frac{\Gamma_\nu}{\Gamma_{\nu,tot}})} \frac{1}{\sqrt{2\pi} \sigma_v} \mathcal{L}'(\nu, \nu'_0) \exp\left(-\frac{v^2}{2 \sigma_v^2}\right) dv \quad (2.29)$$

and

$$\kappa = h\nu n_0 \frac{\alpha_0}{(1 + \frac{2I}{I_s} \frac{\Gamma_\nu}{\Gamma_{\nu,tot}})} \frac{1}{\sqrt{2\pi} \sigma_v} \int_{-\infty}^{\infty} \frac{1}{1 + 4 [\nu - \nu_0 (1 + \frac{v}{c})]^2 / \Gamma_\nu'^2} \exp\left(-\frac{v^2}{2 \sigma_v^2}\right) dv \quad (2.30)$$

The calculation can be performed as in Section 2.6 with the only addition of the power-broadened *width parameter* Γ_ν' . This leads to

$$\begin{aligned} \kappa &= h\nu n_0 \frac{\alpha_0}{(1 + \frac{2I}{I_s} \frac{\Gamma_\nu}{\Gamma_{\nu,tot}})} \frac{1}{\sqrt{2\pi} \sigma_\nu} \frac{\pi \Gamma_\nu'}{2} \exp\left(-\frac{(\nu - \nu_0)^2}{2 \sigma_\nu^2}\right) \\ &= \frac{\kappa_0}{\sqrt{1 + \frac{2I}{I_s} \frac{\Gamma_\nu}{\Gamma_{\nu,tot}}}} \exp\left(-\frac{(\nu - \nu_0)^2}{2 \sigma_\nu^2}\right) \end{aligned} \quad (2.31)$$

and subsequently

$$\kappa = \kappa'_0 \exp\left(-\frac{(\nu - \nu_0)^2}{2 \sigma_\nu^2}\right) \quad (2.32)$$

2.9 Non-linear differential equation

2.10 Data table

		Rubidium	
Isotope	[1]	85	87
Atomic mass	[u]	84.911794	86.909187
10^{-25}	[kg]	1.40999	1.44316
Abundance	[%]	72.17	27.83
Spin I	[1]	$5/2$	$3/2$
Lifetime $6^2P_{3/2}$	[ns]		112
Lifetime $6^2P_{1/2}$	[ns]		125
Wavelength D1-Line ($6^2P_{1/2} \rightarrow 5^2S_{1/2}$)	[nm]	421.5524	
Wavelength D2-Line ($6^2P_{3/2} \rightarrow 5^2S_{1/2}$)	[nm]	420.1792	
$A_{ki,D1}, \Gamma_{\omega,D1}$	[s ⁻¹]	1.50×10^6	
$A_{ki,D2}, \Gamma_{\omega,D2}$	[s ⁻¹]	1.77×10^6	
Natural linewidth $\Gamma_{\nu,D1}$	[MHz]	0.239	
Natural linewidth $\Gamma_{\nu,D2}$	[MHz]	0.282	

Table 2.1 Properties of rubidium isotopes

2.11 D2 line

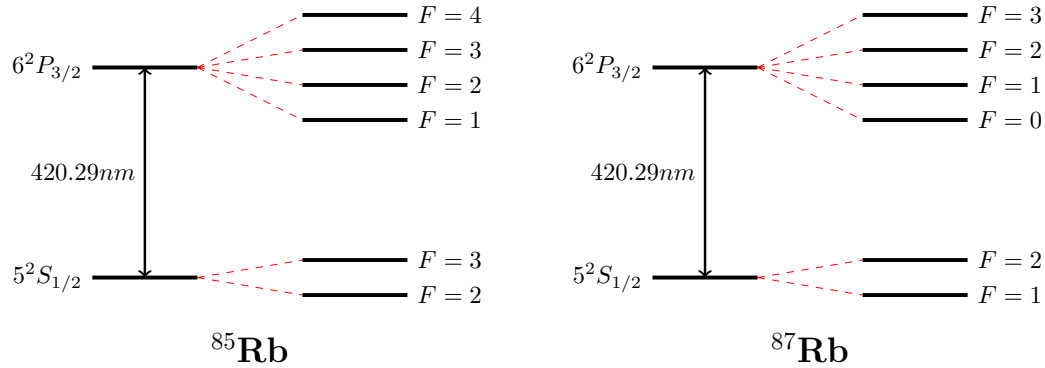


Fig. 2.5 $5^2S_{1/2} \rightarrow 6^2P_{3/2}$ transition of ^{85}Rb and ^{87}Rb with corresponding hyperfine structure

The transition of interest is, as we have discussed before, the $5^2S_{1/2} \rightarrow 6^2P_{3/2}$ of rubidium. As known rubidium occurs in two isotopes, ^{85}Rb and ^{87}Rb . As we can see both isotopes have the same transition energy, but due to the different spin I (see table: 2.1) we get different spin energy levels for the groundstate [8]. This is the reason why we witness four Doppler peaks in our spectrum.

Caution: Both figures below show the correct correlation between energy and isotopes. The reason for this is that the spectrum shows transition energy and the other one the specific energy levels.

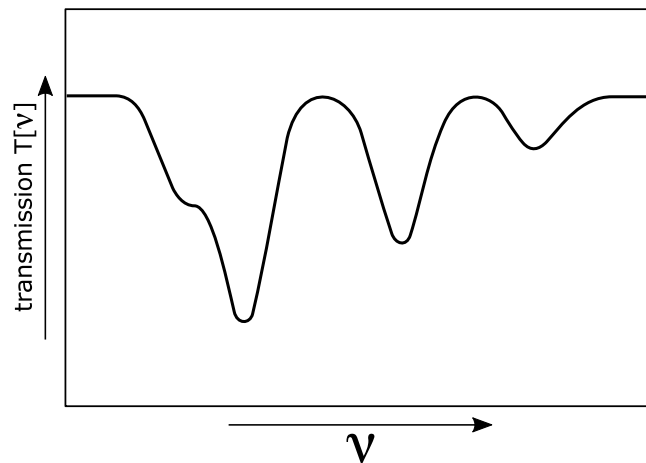


Fig. 2.6 Doppler spectrum of D2 line

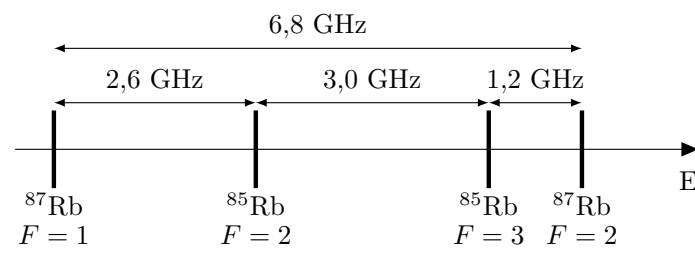


Fig. 2.7 Relative energy gaps of the groundstates between both isotopes

Chapter 3

Experiment

3.1 Setup & Tools

3.2 Laser diameter measurement

3.3 Power / intensity measurement

3.4 Doppler-free measurement

Chapter 4

Evaluation

4.1 Data processing

4.2 Temperature & saturation intensity

4.3 Comparison with theory

4.4 Compare Doppler-free measurement with theoretical values

References

- [1] L.-M. Duan and H. J. Kimble. Scalable photonic quantum computation through cavity-assisted interactions. *Phys. Rev. Lett.*, 92:127902, Mar 2004.
- [2] J. D. Thompson, T. G. Tiecke, N. P. de Leon, J. Feist, A. V. Akimov, M. Gullans, A. S. Zibrov, V. Vuletić, and M. D. Lukin. Coupling a single trapped atom to a nanoscale optical cavity. *Science*, 340(6137):1202–1205, 2013.
- [3] R. Grimm, M. Weidemüller, and Y. B. Ovchinnikov. Optical Dipole Traps for Neutral Atoms. *Advances in Atomic Molecular and Optical Physics*, 42:95–170, 2000.
- [4] Bindiya Arora and B. K. Sahoo. van der waals coefficients for alkali-metal atoms in material media. *Phys. Rev. A*, 89:022511, Feb 2014.
- [5] Danny O’shea. *Cavity QED experiments with a whispering-gallery-mode bottle resonator*. PhD thesis, Vienna University of Technology, ???
- [6] Department of Physics. Saturated absorption spectroscopy. *University of Florida*, 2001.
- [7] Department of Physics. Appendix - saturated absorption spectroscopy. *University of Florida*, 2001.
- [8] J. Reader A. Kramida, Yu. Ralchenko and NIST ASD Team (2015). NIST atomic spectra database (ver. 5.3). *National Institute of Standards and Technology*, 2015.

